

General Disclaimer

One or more of the Following Statements may affect this Document

- This document has been reproduced from the best copy furnished by the organizational source. It is being released in the interest of making available as much information as possible.
- This document may contain data, which exceeds the sheet parameters. It was furnished in this condition by the organizational source and is the best copy available.
- This document may contain tone-on-tone or color graphs, charts and/or pictures, which have been reproduced in black and white.
- This document is paginated as submitted by the original source.
- Portions of this document are not fully legible due to the historical nature of some of the material. However, it is the best reproduction available from the original submission.



This material under NASA sponsorship
is the interest of early and wide dis-
semination of Earth Resources Survey
Program information and without liability
for any use made thereof.

E76-10198

CR-146289

EVALUATION OF SKYLAB PHOTOGRAPHY

FOR

WATER RESOURCES

SAN LUIS VALLEY, COLORADO

by

David Huntley

Remote Sensing Report 75-5

EREP Investigations 380

Contract NAS9-13394

National Aeronautics and Space Administration

(E76-10198) EVALUATION OF SKYLAB
PHOTOGRAPHY FOR WATER RESOURCES, SAN LUIS
VALLEY, COLORADO (Colorado School of Mines)
43 p HC \$4.00

N76-18617

CSCL 08H

Unclas

G3/43-00198

December 1975

REMOTE SENSING PROJECTS

DEPARTMENT OF GEOLOGY

COLORADO SCHOOL OF MINES GOLDEN, COLORADO

EVALUATION OF SKYLAB PHOTOGRAPHY
FOR
WATER RESOURCES
SAN LUIS VALLEY, COLORADO
by
David Huntley


Remote Sensing Report 75-5

Remote Sensing Projects
Department of Geology
Colorado School of Mines
Golden, Colorado

NASA Contract NAS9-13394

National Aeronautics and Space Administration

Approved for Publication:


Keenan Lee
Principal Investigator

December 1975

ABSTRACT

Skylab S190-A and S190-B photography, covering the northern closed basin of San Luis Valley, Colorado, was evaluated with respect to regional water resource studies. Resolution is the most important factor limiting the photography in its use for mapping of surface drainages and hydrologically significant rock units and geologic structures. At the regional level, S190-A stereo photography is sufficient for defining drainage divides and patterns, but is insufficient for hydrogeologic mapping. S190-B photography has adequate resolution to map the hydrogeology in some cases, but aircraft photography is a necessity for most studies and field work is a necessity for all studies, even at the regional level.

Studies of the distribution of vegetation type and saline soils suggest correlation with ground water depth. Narrowleaf cottonwood (Populus angustifolia) trees and willow (Salix spp.) are found where saturated sediments are present within five meters of the ground surface. The distribution of these two vegetation types is best mapped on color-infrared photography. Saline soils are present where the ground water is simultaneously shallow, of relatively high salinity, and potential (head) increases with depth.

Laboratory and field reflectance measurements suggest that band ratioing would not aid in discriminating between moist and dry non-saline soils, but the technique may aid in discriminating saline from non-saline soils.

CONTENTS

	Page
Abstract	ii
Introduction	1
Surface Drainage	3
Hydrogeologic Mapping	7
Lithology	7
Structures	14
Summary and General Remarks	16
Ground Water	17
Vegetation Indicators	18
Saline Soil Indicators	22
Summary and General Remarks	36
Evapotranspirative Discharge	36
Conclusions	37
References	38

FIGURES



Page

1. Outline of water resources study area.	2
2. Drainage map from S190A photography.	4
3. Typical ground water flow patterns	6
4. Effect of irregularities of water table on flow patterns.	8
5. Hydrogeologic map from S190A photography . . .	11
6. Hydrogeologic map.	12
7. Vegetation/land use from Skylab.	20
8. Ground water depth	21
9. Soil salinity distribution from Skylab	23
10. Limit of artesian wells.	25
11. Sodium (alkali) hazard, unconfined aquifer . .	27
12. Sodium (alkali) hazard, confined aquifer . . .	28
13. Salinity hazard, unconfined aquifer.	29
14. Salinity hazard, confined aquifer.	30
15. Bandpass filters used in spectral reflectance measurements	32
16. Normalized band reflectance of dry and moist non-saline soils	32
17. Normalized band reflectance of saline soils, and moist and dry non-saline soils	34
18. Absolute band reflectance of saline and non- saline soils	35

TABLES

1. Skylab photography of San Luis Valley	3
2. Hydrogeologic units of northern San Luis Valley	10

INTRODUCTION

The northern closed basin of San Luis Valley is a major ground and surface water basin of southern Colorado (Fig. 1). Precipitation varies from less than 200mm in the valley to greater than 1200mm in portions of the surrounding mountains. Because of abundant ground water, the San Luis Valley is a major agricultural area of Colorado. The area is currently undergoing extensive exploration for geothermal energy.

Skylab photography of the closed basin was studied to evaluate the potential use of satellite photography as a tool in regional surface and ground water studies. Specifically, the study evaluated the ability of a photo-interpreter, using only Skylab products, to map:

- 1) surface water divides and drainages,
- 2) distribution of hydrogeologically-significant rock and alluvial units, as well as significant structures,
- 3) depth to the ground water table,
- 4) zones of ground water recharge and discharge, and
- 5) areas of relatively high evapotranspirative discharge.

All interpretations were checked by either field work or comparison with ongoing work by the author and work in the San Luis Valley by the U.S. Geological Survey (Emery and others, 1973). All available photography that covered the study area

REPRODUCTION OF THE
ORIGINAL PAGE IS POOR

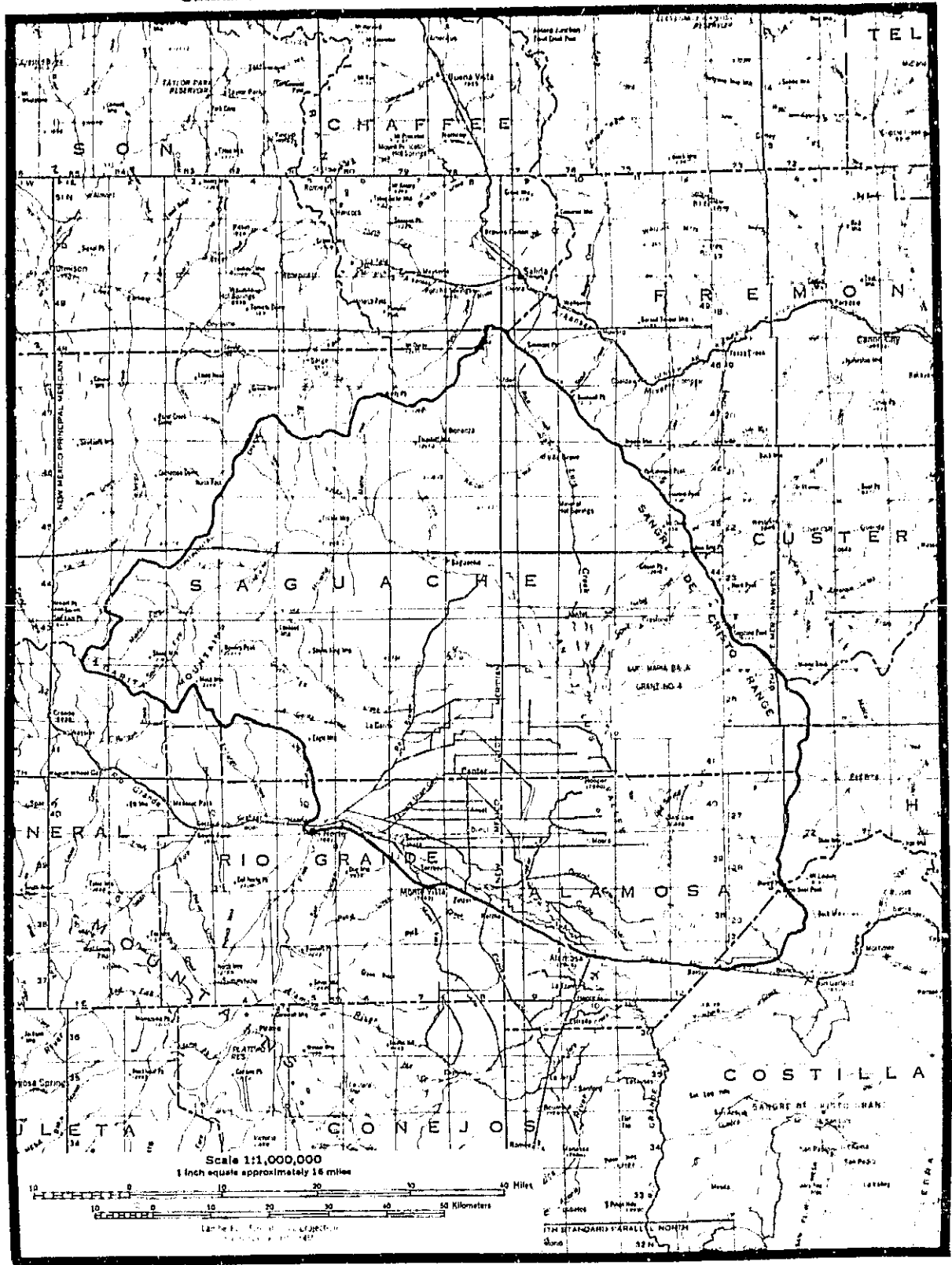


Figure 1. Outline of water resources study area, northern San Luis Valley, Colorado

from Skylab 2, 3, and 4 was interpreted as part of this study and is listed in Table 1.

TABLE 1

Skylab Photography of San Luis Valley

Mission	Date of Acquisition	Track	Frames	Camera System	Comment
Skylab 2	11 June 1973	48	19	S190A	Good
Skylab 3	6 Sept. 1973	30	251	S190A	No stereo coverage
Skylab 3	6 Sept. 1973	30	23	S190B	No stereo coverage
Skylab 3	16 Sept. 1973	30	65	S190A	Cloud covered
Skylab 4	Jan. 1974	34	353,356	S190A	Snow covered
Skylab 4	Jan. 1974	34	98	S190B	Snow covered

SURFACE DRAINAGE

Some of the most important, and certainly some of the most obvious, features observable on Skylab photography are the positions of the major surface water divides and drainages. Figure 2 shows a drainage map of the northeastern part of the study area, as interpreted from Skylab 2 S190A photography. Comparison with Figure 1 shows that the Skylab-prepared drainage map is much more detailed than the existing 1:1,000,000 scale map of the area. Accuracy of the mapped position of the surface water divide is comparable to that of the existing 1:250,000 scale topographic map. The detail of the drainage

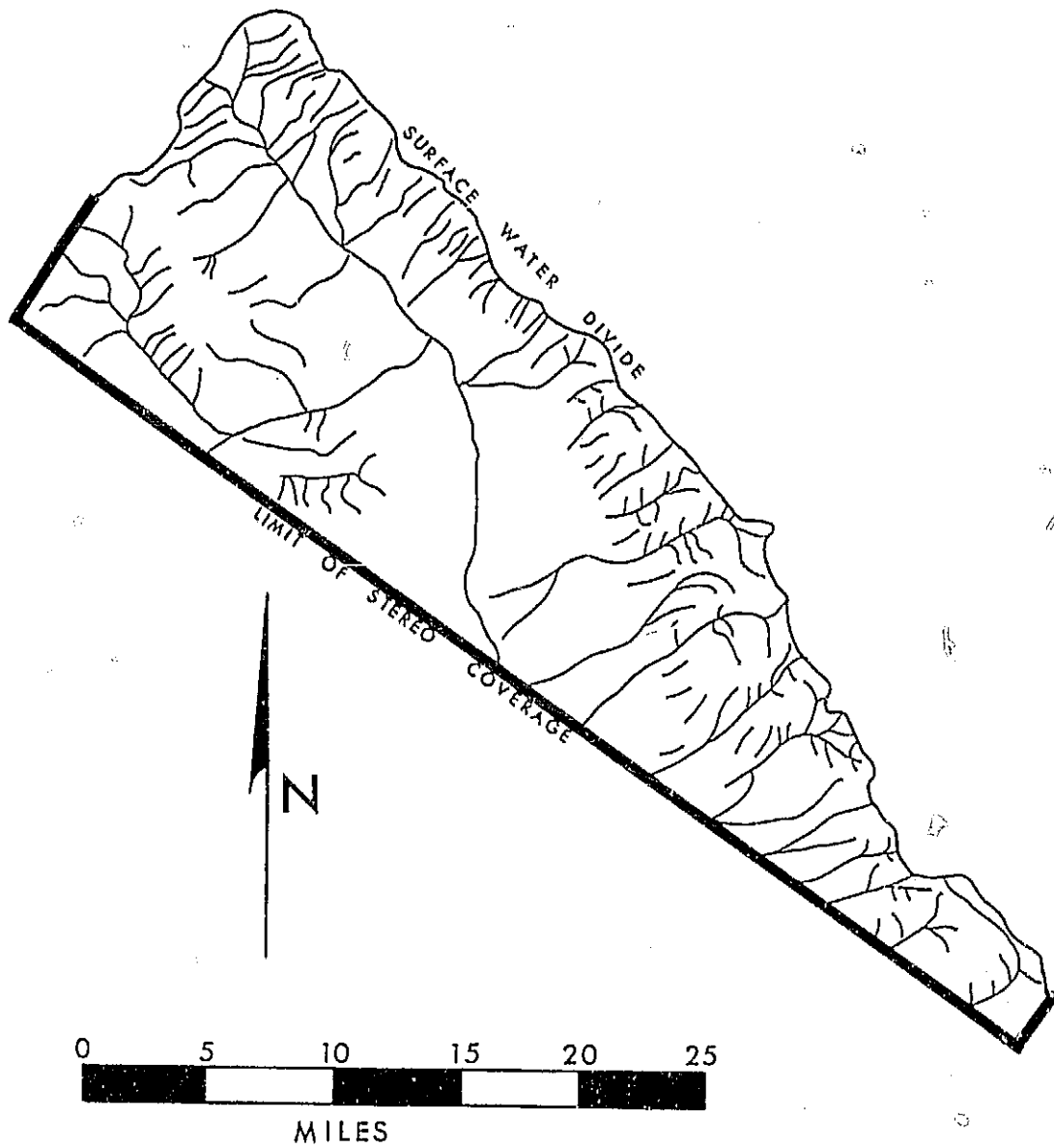
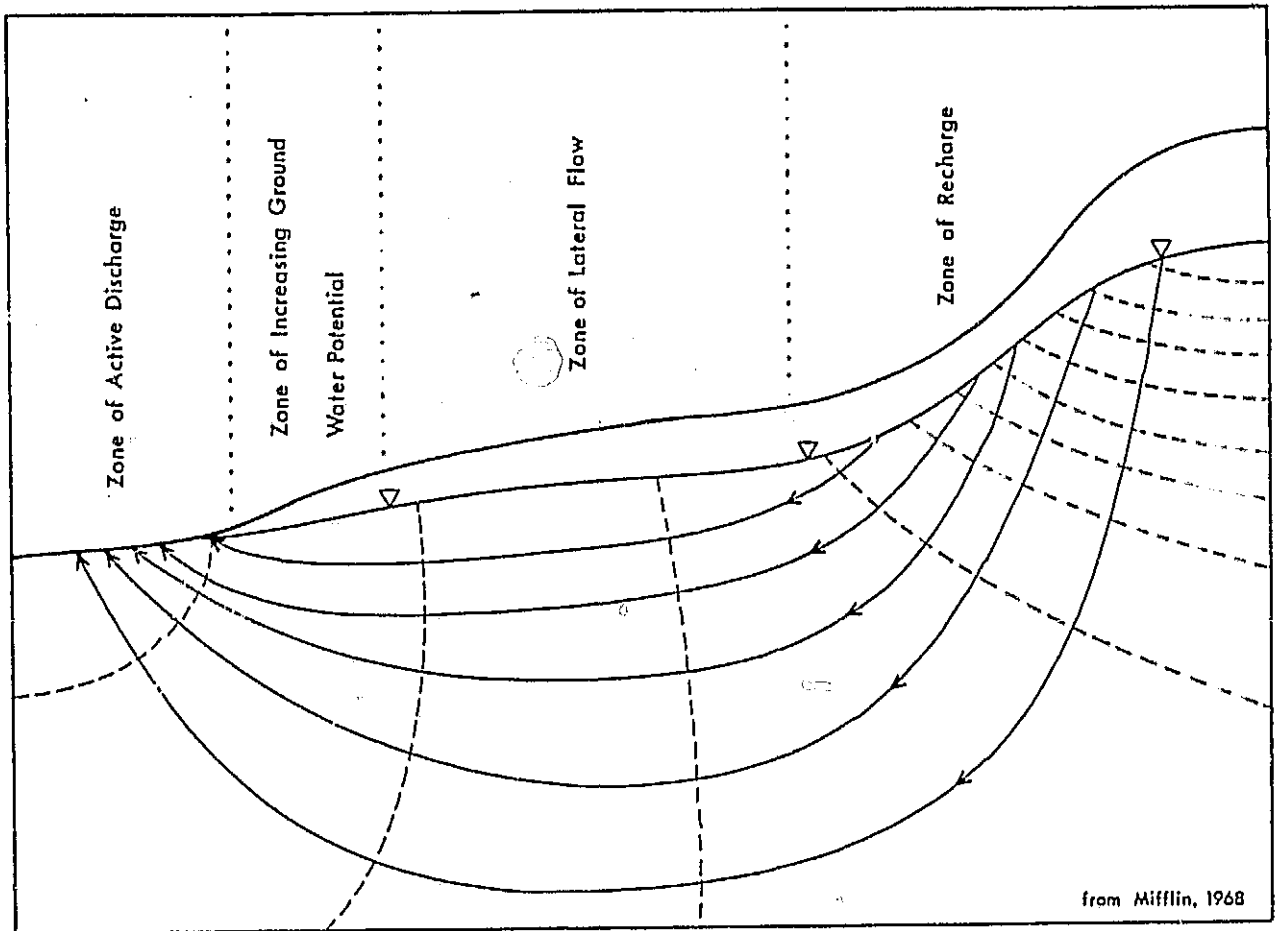


Figure 2. Drainage map of northeastern San Luis Valley drainage basin, as interpreted from Skylab S190A photography.

network, however, is inferior to existing 1:250,000 scale maps. Mapping of the drainage network is best accomplished using color-infrared photography, because streams within the alluvial portion of the basin are best defined by the presence of deciduous vegetation along their course.

Knowledge of the positions of the surface water divide and the drainages is significant not only in the evaluation of surface water flow directions and boundaries, but, in most cases, it helps define the boundaries of ground water movement. In most terrains, the ground water table forms a subdued replica of the topography. Ground water recharge often occurs at topographic highs, and discharge is found at topographic lows (Fig. 3). In a homogeneous medium, or in an inhomogeneous medium of horizontal units, the surface water divides and major drainages will act as impermeable boundaries, and there will be no flow across them. This condition is approached in the San Luis Basin, where rocks west of the valley are near-horizontal, alluvium within the valley is near-horizontal, and indurated rocks east of the valley are fractured in a homogeneous manner. Because these conditions are met, the surface water divide shown in Figure 2 also acts as a ground water divide and the fourth-order stream shown (where a first-order stream is defined as one with no tributaries) is the center of discharge for both the unconfined and confined aquifers present within San Luis Valley. In addition, both Toth (1963) and Freeze (1969)



- equipotential lines
- ← flow lines
- ▽— water table
- ground surface

Figure 3. Typical ground water flow patterns.

have shown that lower-order streams may define areas of discharge for more local ground water flow systems. Figure 4 shows the influence of ground water table irregularities on the flow system. A local flow system is one whose areas of recharge and discharge are immediately adjacent.

In summary, the resolution of Skylab S190A photography is adequate to define the major drainage divides and streams, as well as several lower-orders of streams. If the rocks of the region can be approximated as either a homogeneous medium or a horizontally-bedded, inhomogeneous medium, and if the water table configuration follows topography, then the drainage information available on Skylab photography defines ground water flow boundaries and the extremities of the regional and local recharge/discharge system. It can be seen that the first assumption can be evaluated by mapping the significant hydrogeologic units.

HYDROGEOLOGIC MAPPING

Lithology

Rock types in the San Luis Basin include fractured Precambrian igneous and metamorphic rocks and Paleozoic sedimentary rocks of the Sangre de Cristo Mountains, Tertiary volcanic rocks of the La Garita Mountains, and extensive Quaternary alluvial deposits lying on a thick section of Tertiary sediments and volcanics in the San Luis Valley. A

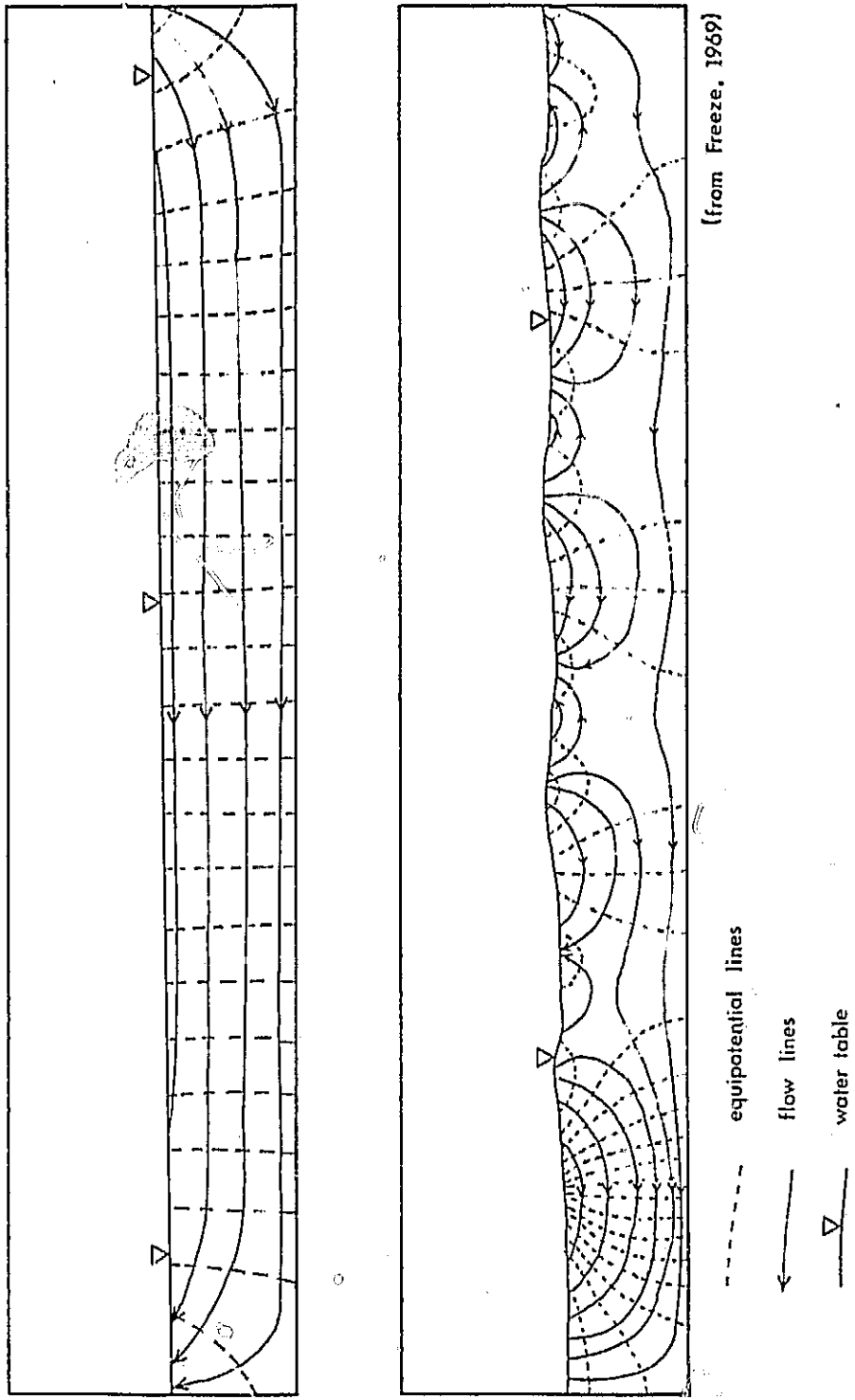


Figure 4. Effect of irregularities of the water table on local and regional flow systems.

description of the hydrogeologic properties of these rocks is presented in Table 2.

Skylab 2 S190A photography covering the northeastern part of San Luis Valley was chosen for the most complete hydrogeologic photointerpretation because it is the only cloud-free, snow-free photography with stereo coverage over the area. Other photography was interpreted in a less complete fashion and will be discussed later. Figure 5 shows the hydrogeologic photointerpretation. For comparison, Figure 6 shows the completed hydrogeologic map covering a portion of the same area as Figure 5. The towns of Villa Grove and Crestone are on both maps for location. The completed hydrogeologic map is the result of interpretation of satellite photography and imagery, aircraft high-and low-altitude photography and imagery, and extensive field work.

Drainage patterns and topographic expression are the most important features used to discriminate rock and alluvial units in the basin. With the exception of the most recent stream deposits, which are identified by their associated deciduous vegetation, spectral differences between units is unimportant in discrimination. Resolution is therefore the most important film characteristic in hydrogeologic mapping of the region. Because of the arid climate of San Luis Valley, drainage patterns on the alluvial fans are relatively small-scale, and are generally below the resolution of both the S190A color and color infrared photos. Alluvial fan units

TABLE 2
Hydrogeologic Units of Northern San Luis Valley

Hydrogeologic Unit	Description	Type of Permeability	Hydraulic Conductivity (Darcys)
Recent stream Deposits	Ranges in texture from silt-size through cobble and boulder-size. Permeability varies downstream and with age of alluvial unit it crosses.	Intergranular	0.001-60
Eolian Sands	Moderately well-sorted to well-sorted sands forming both active and stabilized dunes.	Intergranular	5-20
Quaternary Alluvial Fans	4 Small, steeply sloped, most recent fan. Poorly sorted with continuous grain-size gradation of silt through cobble.	Intergranular	0.1-5
	3 Relatively well-sorted deposits with grain size varying from fine-sand to cobble-size. Largest of the alluvial fans.	Intergranular	12-40
	2 Medium to coarse-grained, poorly to moderately well-sorted. The slope is intermediate between units 1 and 3 and is moderately dissected.	Intergranular	30-60
	1 Oldest alluvial fan unit in sequence; Very steep and highly dissected. Caliche layer near top of unit is very coarse-grained.	Intergranular	55
Valley Fill	Wide range of textures, grain-sizes, degrees of cementation.	Intergranular	<0.00001-60
Youngest Volcanics	Andesite and basalt flows.	Fracture, constant with depth.	0.9-100
Uppermost Ash-flow Sequence	Quartz latite to rhyolite ash-flow tuffs. Degrees of welding vary from unwelded to highly welded. Permeability is greatest in highly welded portions. Permeability is strongly anisotropic.	Fracture, constant with depth.	30-60
Middle Ash-flow Sequence	Includes Carpenter Ridge Tuff (Rhyolite), Fish Canyon Tuff (Quartz latite), and thin andesite flow. Permeability is strongly anisotropic and is greatest in highly welded tuffs.	Fracture, constant with depth.	1-100
Upper Air-fall/Water-laid Tuff	Fine grained, unwelded tuffs.	Intergranular	0.00001-0.01
Sapinero Mesa Tuff	Rhyolite ash-flow tuff.	Fracture, constant with depth	30-40
Lower Air-fall/Water-laid Tuff	Fine grained, unwelded tuffs.	Intergranular	0.00001-0.01
Conejos Formation	Rhyolite to basalt (dominantly andesite) flows, flow breccias, air-fall/water laid tuffs, laharic breccias.	Intergranular and fracture, constant at depth	0.00001-3
Tertiary Intrusives	Intermediate to silicic intrusives of early Tertiary age.	Fracture	0.001-0.01
Basement	Paleozoic sandstones, shales, conglomerates, limestones, all very well indurated, and Precambrian schists, gneisses, and granodiorite intrusives.	Fracture, decreasing with depth	0.001-0.1

**REPRODUCTION OF THE
ORIGINAL FILE IS POOR**

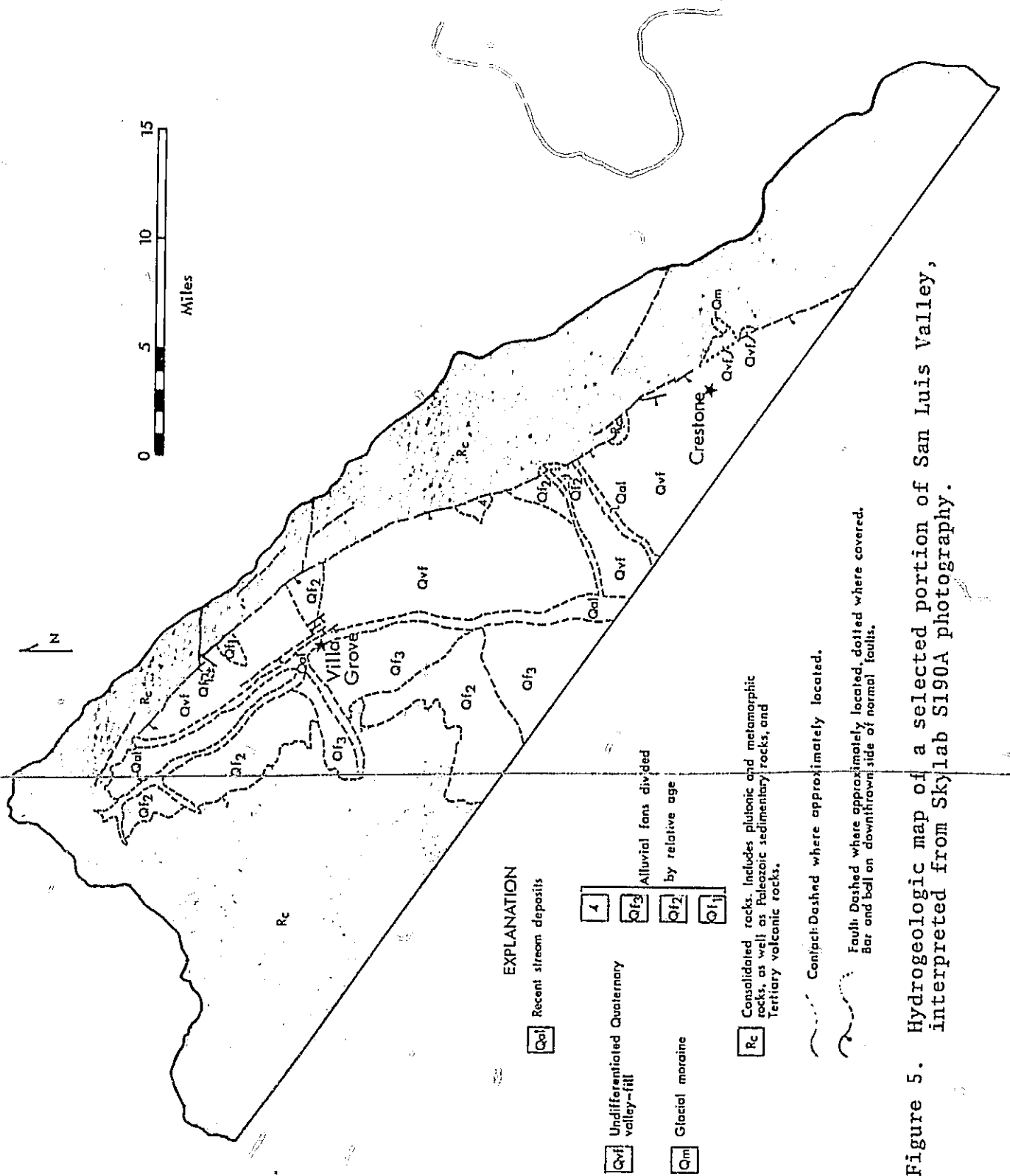


Figure 5. Hydrogeologic map of a selected portion of San Luis Valley, interpreted from Skylab S190A photography.

REPRODUCIBILITY OF THE ORIGINAL PAGE IS POOR

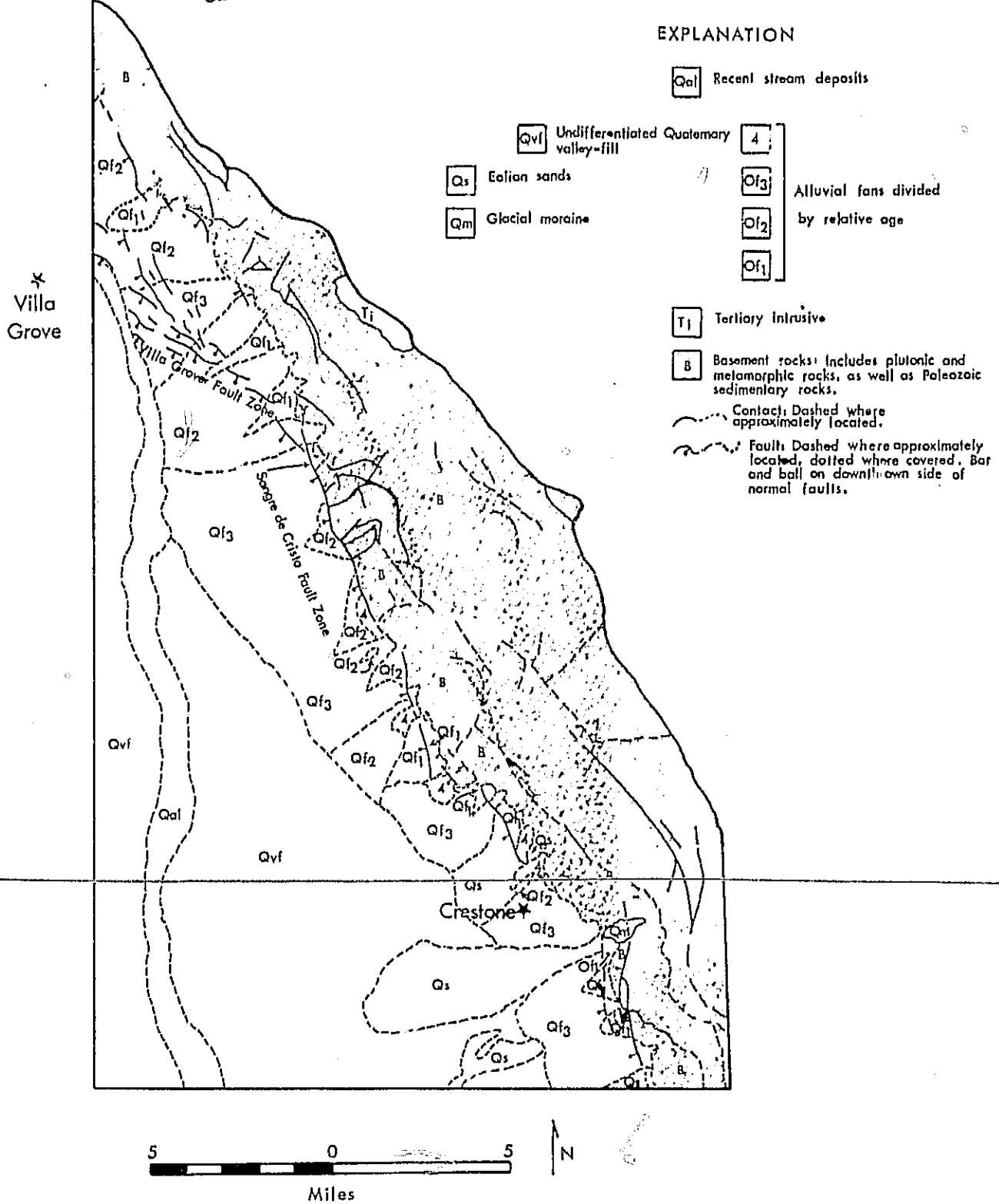


Figure 6. Hydrogeologic map of a selected portion of the San Luis Valley.

can be discriminated only where differences in extent and slope are detectable. Stabilized eolian deposits similarly are not discriminable from other low-lying alluvial units because the sand dunes (visible on larger-scale photography) are below the resolution capability of the S190A camera system. Though no stereo coverage exists for the Skylab 3 S190B September photos, it is nonetheless apparent that the increased resolution of the system increases information content. Drainage textures on the alluvial fans south of Crestone are well within the resolution capability of the S190B. It is very likely that, with stereo coverage, a complete subdivision of alluvial units would be possible, suggesting that mapping at reconnaissance-level accuracy could be achieved in alluvial areas using only S190B photography.

Discrimination between the basement sequence of fractured crystalline and sedimentary rocks and Tertiary volcanic rocks of the Conejos Formation is not possible with any of the S190A photos. ~~This is due largely to the thick stands of~~ coniferous vegetation in both the Sangre de Cristo Mountains and the La Garita Mountains/Bonanza area. Bedding within the Conejos Formation is below the resolution capability of the S190A system, and so cannot be used as a basis for discrimination. Drainage density may be somewhat greater in the basement complex than within the Conejos Formation, but the relationship is by no means consistent.

Only snow-covered photography is available to study terrain covered by post-Conejos Formation volcanic rocks. In general, terrain underlain by ash-flows can be recognized by the flat-top plateaus and the regular joint patterns developed in the welded ash-flows. The only unit within this sequence that can actually be identified relatively consistently is the Fish Canyon Tuff. It should be noted, however, that many of the same comments can be made about conventional low- and medium-altitude aircraft photography.

Volcanic units in this region lack any distinctive spectral contrasts and can be mapped only by their topographic expression. Correlation based on topographic expression is extremely tenuous because of the control of pre-existing topography on the distribution of volcanic rocks. Any mapping of volcanic rocks is likely to require extensive field work. Resolution is again the major factor in the interpretation of the volcanic units; S190B photography permits a more detailed subdivision of rock units than does the S190A photography.

Structures

Geologic structure, particularly faults, exerts a strong influence on ground water movement in the San Luis Basin. Fractures provide the most significant permeability in the marginal bedrock units, and fractures are much more closely spaced and more pervasive in the vicinity of faults, despite the fact that the faults themselves may exhibit little or no

permeability because of gouge developed from relative shear motion. Faults within the alluvial sequence of San Luis Valley often are ground water barriers, probably because of the development of gouge along the fault plane.

Faults within the Sangre de Cristo Mountains and the Bonanza area can be interpreted only by the presence of linear topographic depressions, or the linear alignment of discontinuous topographic depressions, such as ridge saddles. The capability of mapping stratigraphic units in sufficient detail to delineate fault separations is simply not present using S190A system photography. The majority of faults in the basement complex shown in Figure 6 have been mapped on the basis of stratigraphic information, and are therefore not delineated in Figure 5, the Skylab S190A interpretation. All faults shown in Figure 5 can be correlated with real faults in the field, although often a single fault mapped on Skylab photography correlates with a complex series of faults on the ground.

~~The two major fault zones in the area are the Sangre de~~
Cristo fault zone, trending northwest and separating the basement complex from the Quaternary alluvium, and the Villa Grove fault zone, trending northwest between Villa Grove and Sangre de Cristo fault zone. Both zones are a series of en echelon normal faults. Fault scarps within the alluvium of up to 10m in height are found along both fault zones. Comparison between the interpretation of S190A photography (Fig. 5) and the final hydrogeologic map (Fig. 6) shows that

interpretation of the Sangre de Cristo fault zone on Skylab photography is generalized, and interpretation of the Villa Grove fault zone is nearly absent. This difference is solely a function of the resolution of the photographic system. The mapping of the Sangre de Cristo fault zone is not based on the presence of fault scarps in the alluvium except along isolated segments. The photointerpretation of the fault is based primarily on the position of the sharp, linear break between the basement complex and the alluvium of San Luis Valley. Only the segment of the Sangre de Cristo fault due north of Crestone is visible on S190A photography as an alluvial fault scarp. It should be noted that it is only visible on the color and red-band photography, because of the superior resolution of these systems.

The Villa Grove fault zone is visible only near the town of Villa Grove, and is interpretable there only because of the heavy deciduous vegetation developed on the up-gradient side of the fault in response to ground water ponding. Without the capability to map fault-scarps in the alluvium, however, there is little to suggest the continuation of a fault zone between Villa Grove and the Sangre de Cristo fault.

Summary and General Remarks

Resolution of the film/camera system is the most important factor determining the amount of hydrogeologic information that can be interpreted. The S190A system does not have sufficient

resolution for more than a cursory examination of the distribution of rock and alluvial units. Though no stereo coverage was available for the S190B system, it is still obvious that much more information results from the greater resolution. Interpretation of stereo S190B photographs would probably produce a map comparable to that of an interpretation of high-altitude aircraft photography, sufficient for a reconnaissance-level, regional ground water study. Because resolution is the most important factor in interpretability, the films with the greatest resolution contain the most information, except where vegetation information is important (such as the fault scarps near Villa Grove). The red and green bands of the S190A contain the same information as the color band, though the resolution of the red band may be somewhat superior to that of the green band. Both of the infrared bands and the color infrared band have inferior resolution. The color infrared film is useful for vegetation-related rock distribution or structure, while the black and white infrared bands contain little useful information because of the extreme graininess of the film.

GROUND WATER

Two approaches were followed in an attempt to determine ground water depth and quality using Skylab photography. The first approach consists of determining the relationship between vegetation type and density and ground water depth and

quality, and then evaluating the minimum contrast between vegetation zones that is identifiable using S190A color or color infrared photography. The second approach is an attempt at relating saline soils, which appear as areas of high reflectance on photography, to ground water depth and quality.

Vegetation Indicators

Previous studies (Huntley, 1973) in the San Luis Valley have indicated several relationships between ground water depths and vegetation type and density. These relationships are observable both in the field and on low-altitude color-infrared photography, and include:

1) Thick stands of narrowleaf cottonwood (Populus angustifolia) trees where the water table is less than five meters from the surface, and thin stands of narrowleaf cottonwood trees that are restricted to the immediate vicinity of an active stream where the ground water table is greater than five meters deep and where shallow, water-saturated sediments are restricted to the stream bank sediments. Narrowleaf cottonwood trees are restricted to areas of good water quality.

2) Growths of willow (Salix spp.) occur under the same conditions as narrowleaf cottonwood trees, but they are not restricted to areas of high water quality.

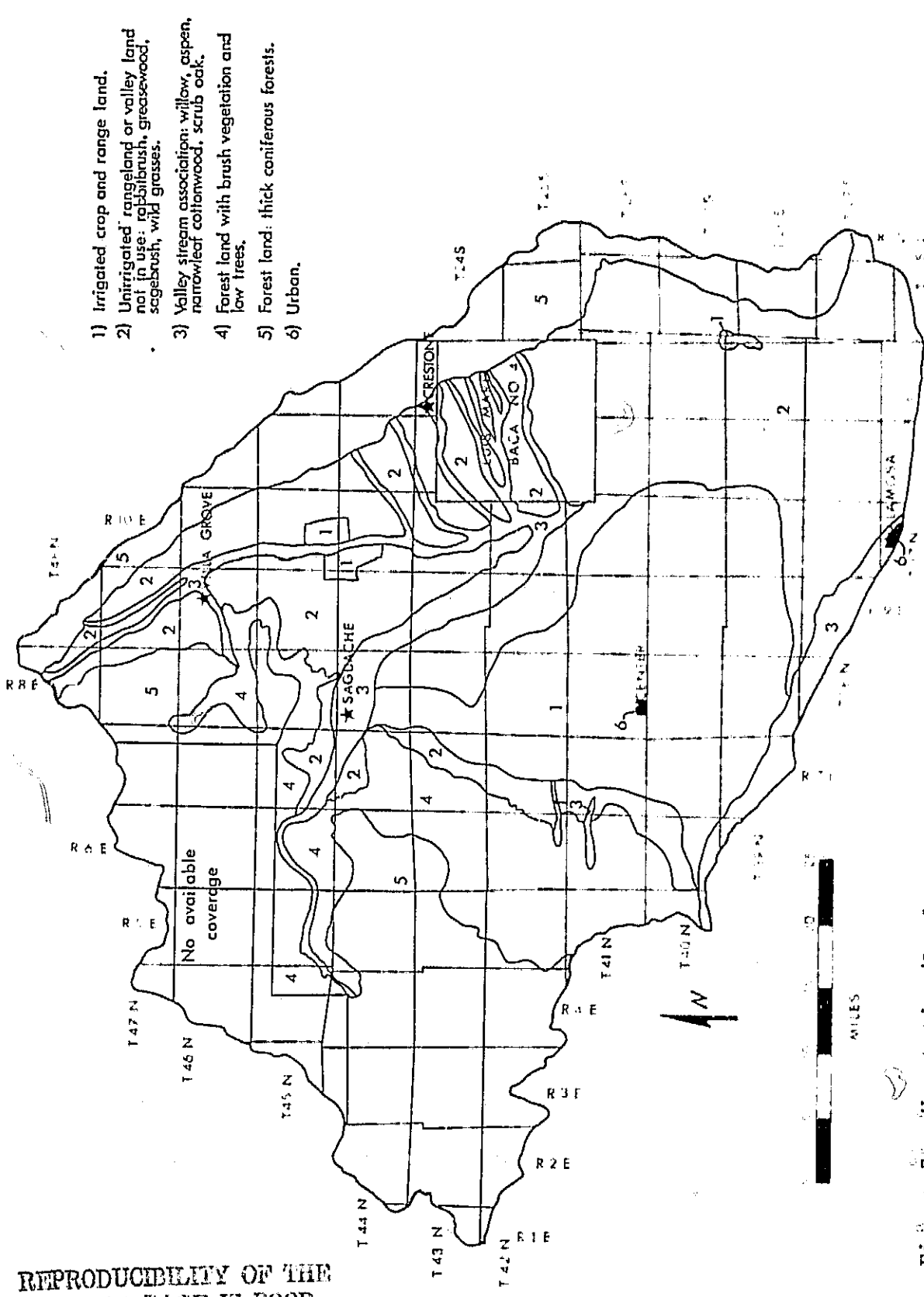
3) The density of rabbitbrush (Chrysothamnus nauseosus) can sometimes, but not consistently, be correlated with ground water depth. Dense growths usually are related to ground water depths of less than seven meters, but shallow ground water may exist without a dense growth of rabbitbrush.

4) Wiregrass (Juncus balticus) commonly is found in areas where the water table is less than one meter from the surface and periodically reaches the surface.

5) Other brush-type vegetation, such as saltbush (Atriplex canescens) and greasewood (Sarcobatus vermiculatus), have an irregular and unpredictable relation with ground water depth. High density often is related to shallow ground water, but the converse is not consistently true.

Of the above relations, only the first two are observable on Skylab photography, because of their high photo-infrared reflectance. Figure 7 shows a vegetation/land use map derived from interpretation of Skylab 3 S190A color-infrared photography, and Figure 8 shows a ground water depth map from Emery and others (1973). Throughout much of the area, a fairly strong correlation exists between shallow ground water (<2m) and the stream-associated vegetation. The correlation breaks down where agricultural practices have eliminated the natural vegetation or where water quality is very poor.

Unfortunately, the vegetation associations of narrowleaf cottonwood and willow also exist in areas where the water



- 1) Irrigated crop and range land.
- 2) Unirrigated rangeland or valley land not in use: rabbitbrush, greasewood, sagebrush, wild grasses.
- 3) Valley stream association: willow, aspen, narrowleaf cottonwood, scrub oak.
- 4) Forest land with brush vegetation and low trees.
- 5) Forest land: thick coniferous forests.
- 6) Urban.

REPRODUCIBILITY OF THE ORIGINAL PAGE IS POOR

Figure 7: Vegetation/land use interpreted from Skylab.

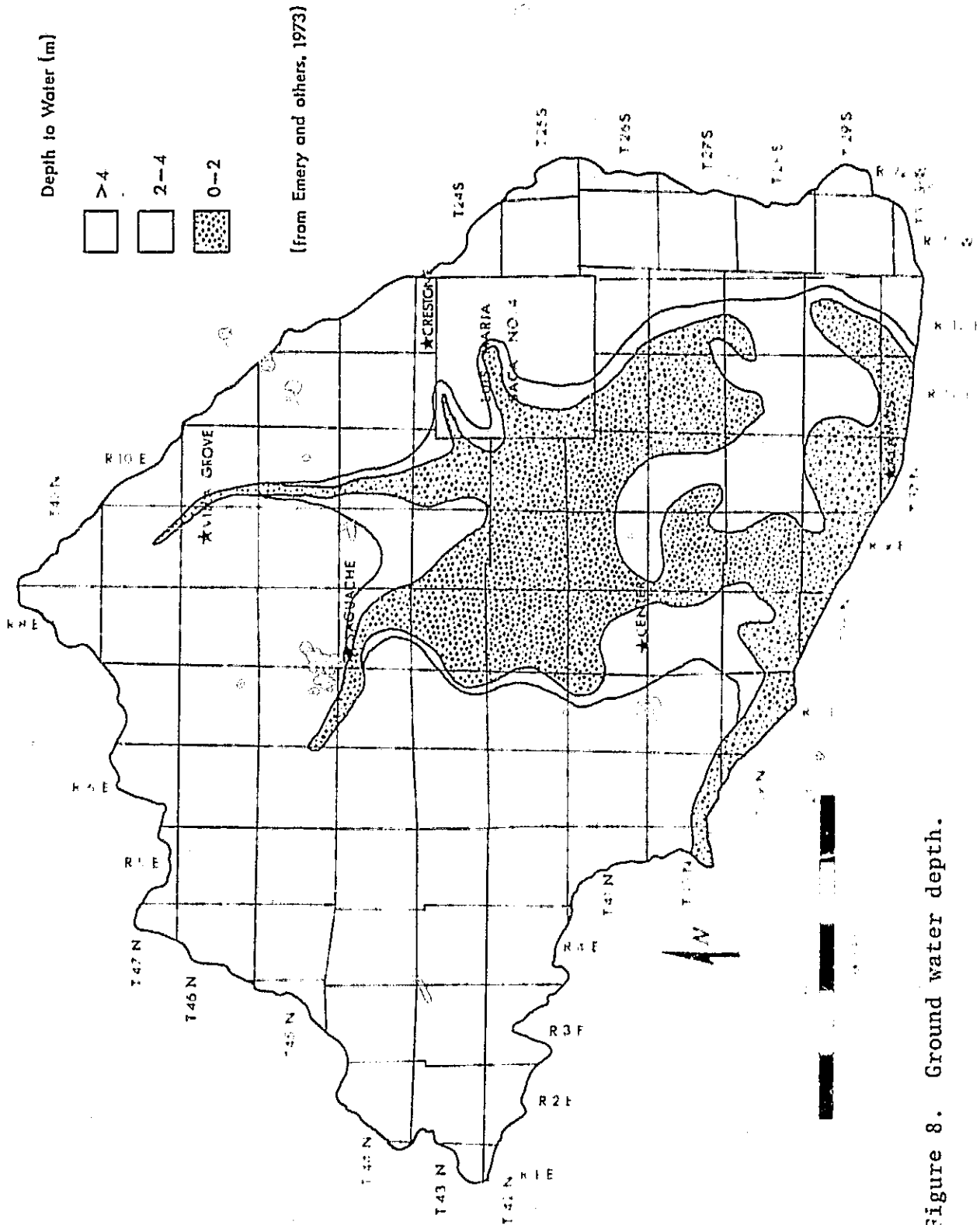


Figure 8. Ground water depth.

table is greater than 4m, as indicated by Limery and others (1973). This occurs in areas where stream flow is high enough throughout the year to keep stream bank sediments saturated, and where perched water tables exist. Areas of perched water tables cannot be discriminated from areas where the real water table is shallow, but the above two often can be discriminated from areas where only the stream banks are saturated by examining the distance that the vegetation has grown away from streams.

Density variations within the brush-type vegetation are not observable with the available resolution of the S190A system.

Saline Soil Indicators

Possible relations between saline soil and ground water depth were first observed on LANDSAT imagery and studied in more detail on Skylab 3 S190A photography. The distribution of saline soils was mapped from S190-A photography (Fig. 9) and was studied to determine its relation to ground water depth, quality, and direction of flow. Reflectances of dry saline soils and moist and dry non-saline soils were measured to determine the best method for isolating the saline soils on photography.

Comparison of the interpreted soil salinity (Fig. 9) with ground water depth (Fig. 8) shows that saline soils develop only where the ground water is relatively shallow, but that saline soils are not present everywhere the ground

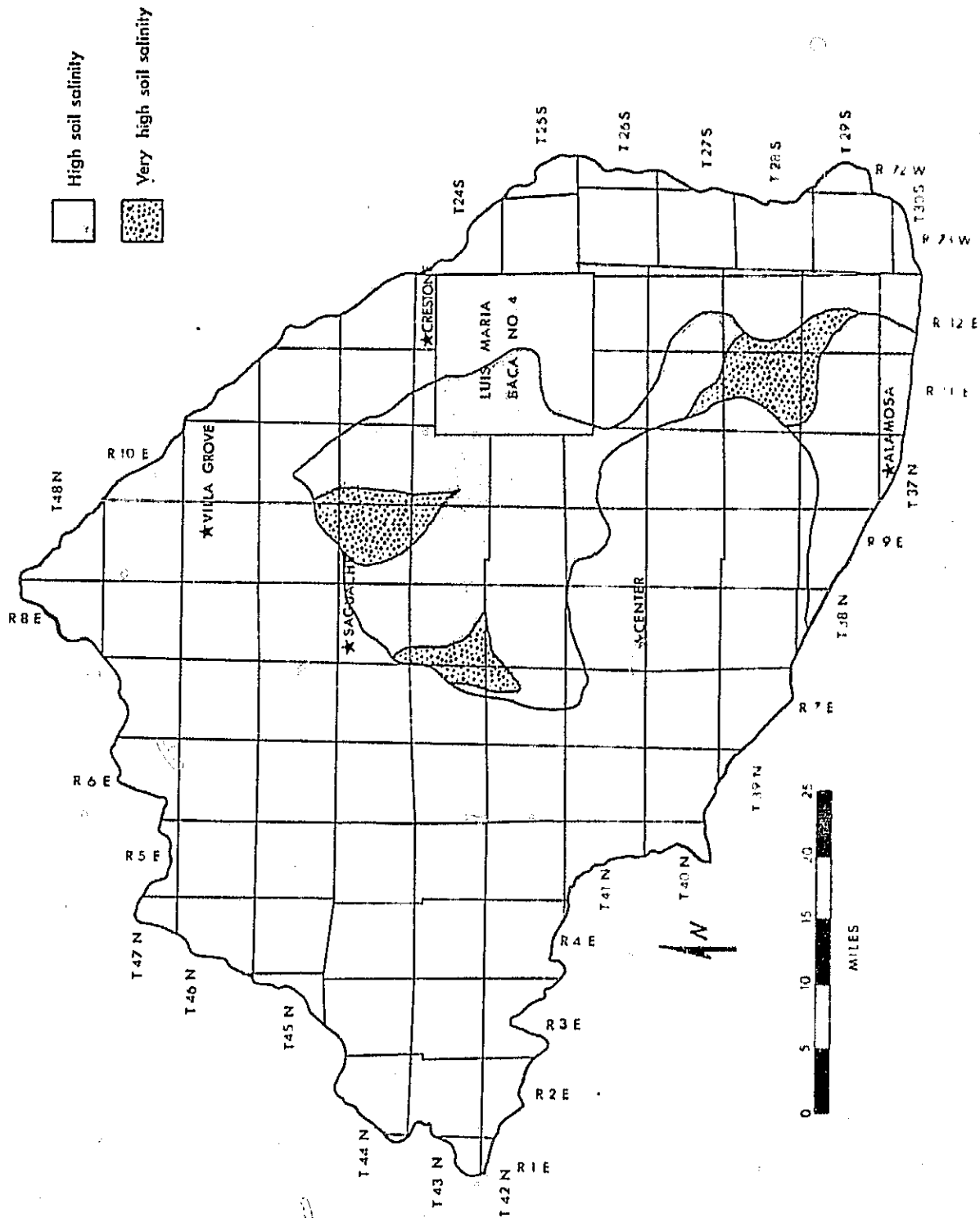


Figure 9. Soil salinity distribution interpreted from Skylab.

ORIGINAL PAGE IS
OF POOR QUALITY

water table is near the surface. Saline soils are not present, or are masked, in areas of agricultural land use, as seen when the saline soils distribution is compared with the vegetation/land use map (Fig. 7). Overhead irrigation in agricultural areas tends to rinse the soil free of heavy surface accumulations of salts and, at the same time, the agricultural crops tend to hide soils at the resolution of satellite photography.

The presence of shallow ground water associated with non-saline soils indicates that at least one additional parameter limits the distribution of saline soils. Water quality, and the position of the saline soils within the ground water recharge/discharge system were both considered. Figure 10 shows the limit of artesian wells in San Luis Valley. As artesian conditions are produced by an increasing ground water potential (or head) with depth, flowing wells are found only in areas of potential ground water discharge. The confined and unconfined aquifers of San Luis Valley exhibit a great deal of interaquifer communication, and it is likely that the boundary of the area of potential ground water discharge for the confined aquifer is nearly coincident with the boundary of potential ground water discharge for the shallow, unconfined aquifer. All areas of high soil salinity can be represented as areas of shallow ground water within the zone of potential discharge. The northern and eastern boundaries of shallow ground water and ground water discharge

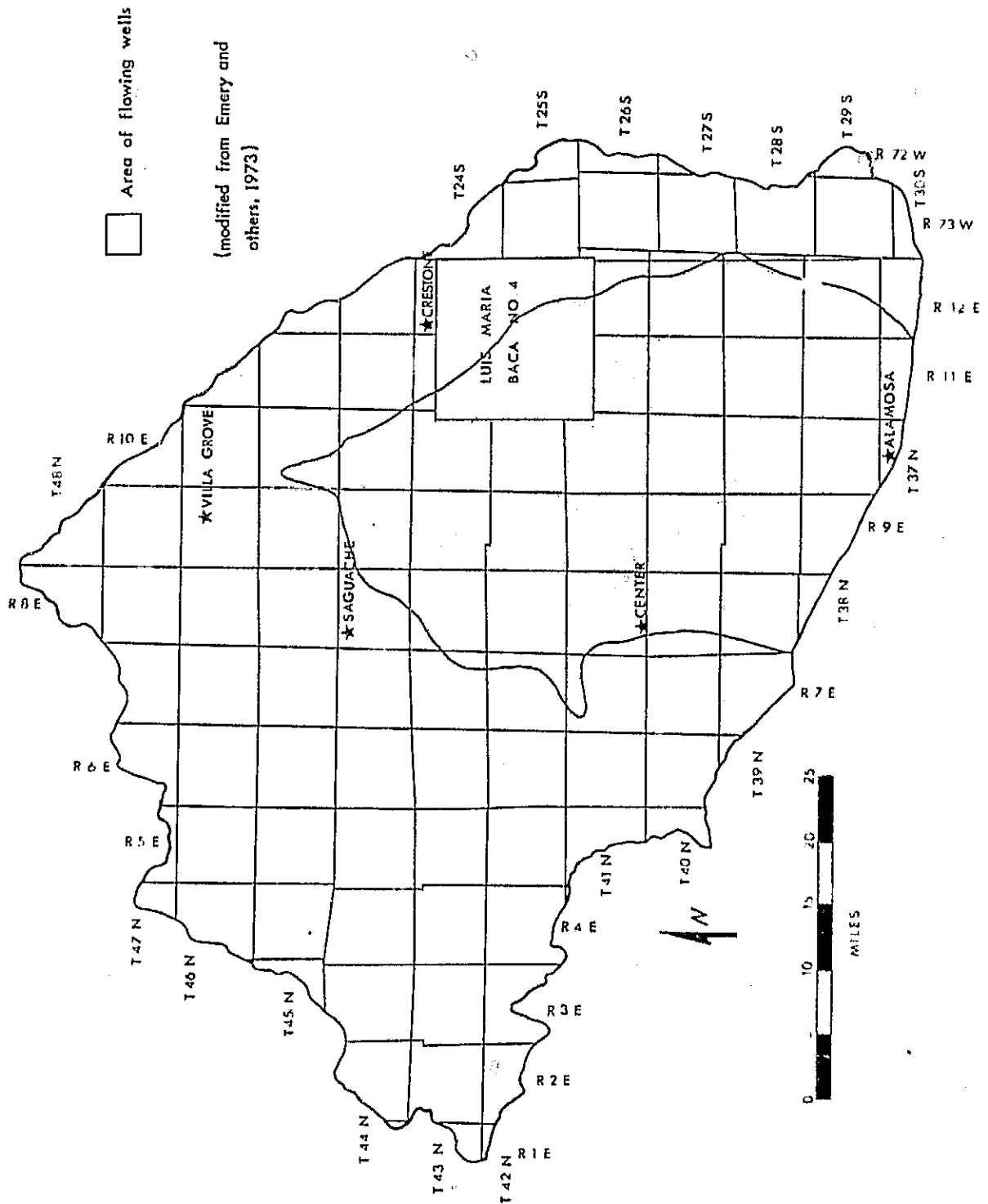


Figure 10. Limit of artesian wells.

correlate particularly well with the limits of soil salinity. The areas of very high soil salinity and the eastern boundary of soil salinity are not explained by even a combination of potential ground water discharge and shallowness.

Figure 11 through 14 show the distribution of salinity and sodium hazard for both the confined and unconfined ground waters of San Luis Valley. The area of very high soil salinity centered on T.39N., R.11E. is in the center of the closed basin sump, the central area of ground water discharge for the closed basin. Salinity and sodium hazards for the unconfined aquifer are extremely high in this area, and evaporation of this water produces soils of extremely high salinity. The area of very high soil salinity centered on T.43N., R.8E. is a region of surface springs and heavy artesian well usage. Evapotranspiration is heavy in this region, and accumulation of salts in the soil results. The area of very high soil salinity centered on T.44N., R.9E. is an area where evaporation from the water table (at a depth of 2-4m) is minimal, but artesian wells are used heavily and evaporation from accumulated surface water is substantial. The westward flexure of the soil salinity boundary near the southern boundary of the Luis Maria Baca No. 4 correlates well with areas of relatively high water quality in both the unconfined and confined aquifers.

Areas of high soil salinity appear to correlate relatively well with areas of shallow, discharging ground water that

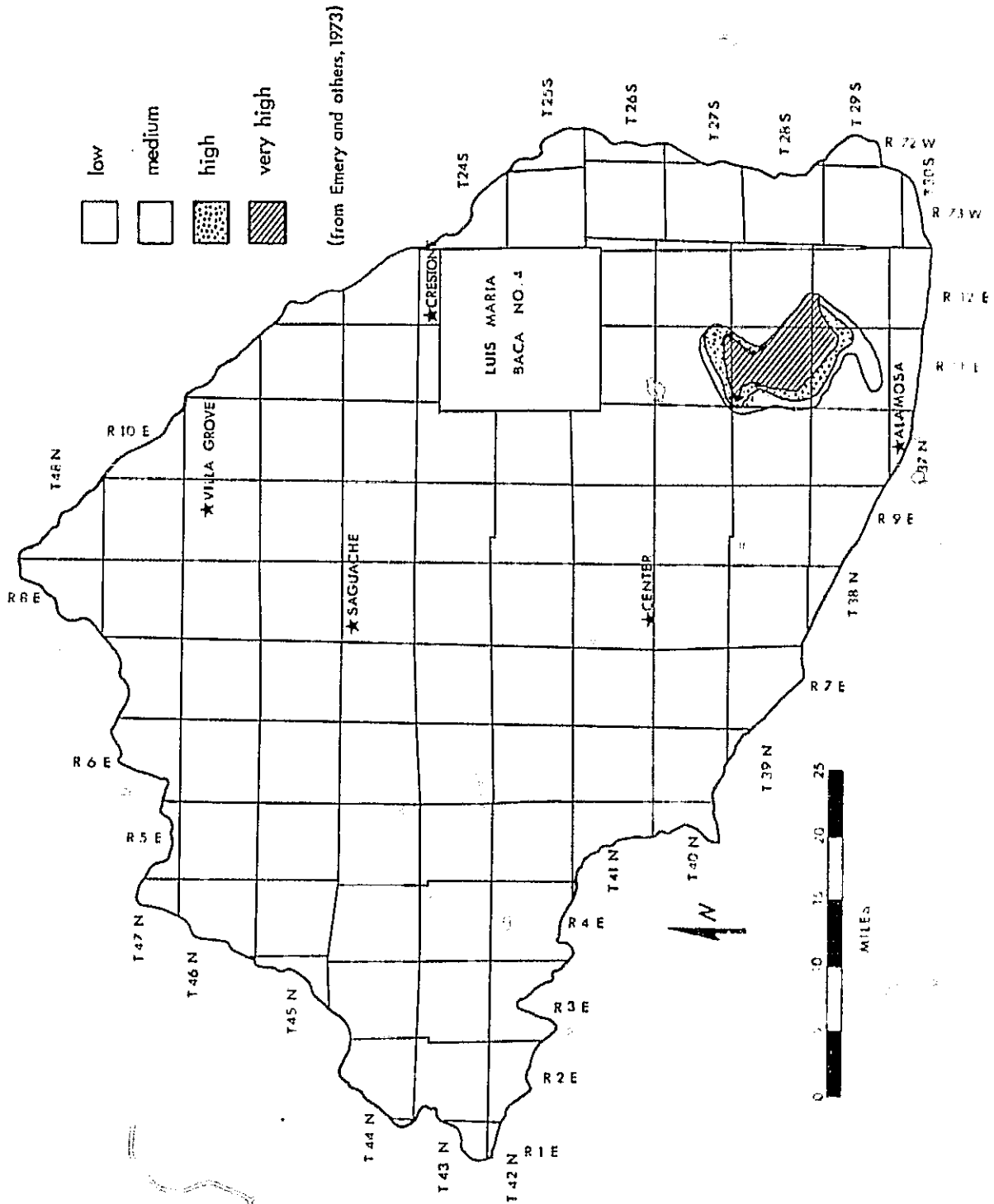


Figure 11. Sodium (alkali) hazard, unconfined aquifer.

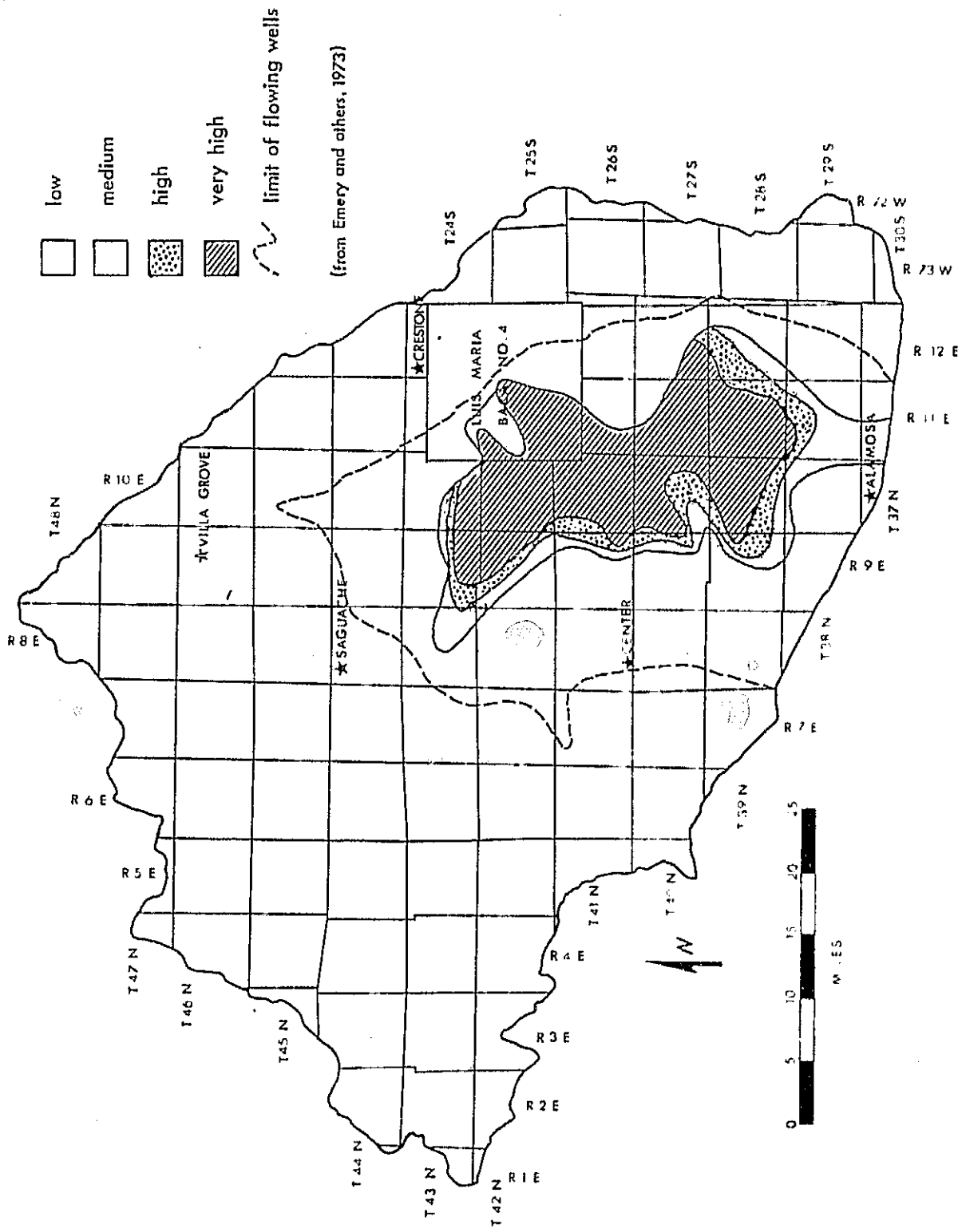


Figure 12. Sodium (alkali) hazard, confined aquifer.

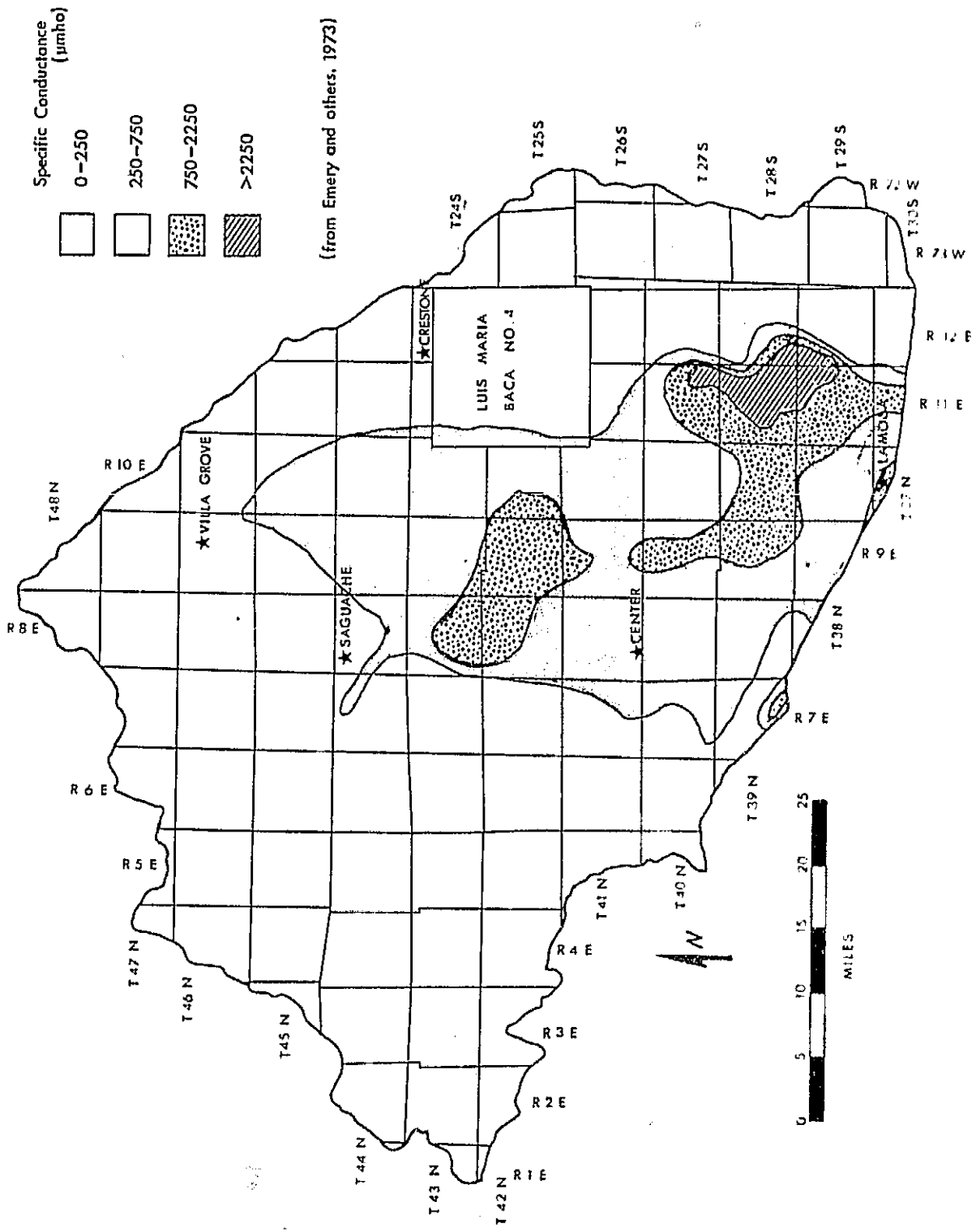


Figure 13. Salinity hazard, unconfined aquifer.

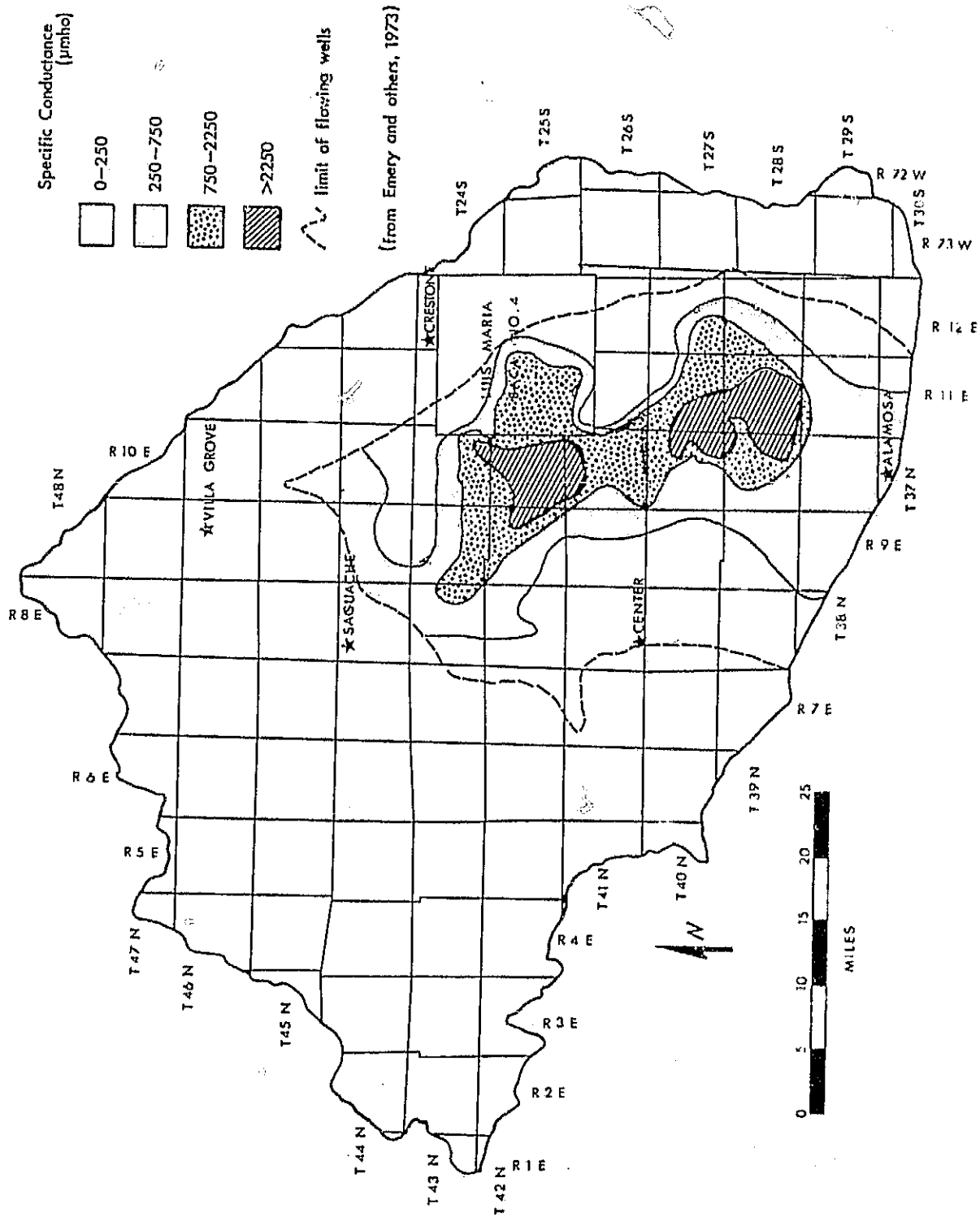


Figure 14. Salinity hazard, confined aquifer.

contains at least a moderate concentration of salts. The use of soil salinity in the interpretation of ground water depth appears to be more dependable than vegetation, if interpreted with care. With this in mind, examination of the spectral reflectance of the saline soils was undertaken to attempt to better delineate these soils.

Saline soil reflectances were measured in the field only, while dry and moist non-saline soil reflectances were measured in both the laboratory and field. The saline soils are dominantly very fine-grained silts and clays, while the non-saline soils range from clay through wind-blown sands, organic-rich peats, and cobble-strewn alluvium.

Reflectance measurements were made using the filter wheel photometer described by Raines and Lee (1974). Measurements were made in 13 spectral bands covering the photographic region (Fig. 15). To determine if band ratioing (Raines and Lee, 1975) might be a successful technique, the data were computed as normalized band reflectances by dividing all band reflectances values by the corresponding no-filter band reflectance value. This technique shows whether there is any significant difference in the shape of the spectral reflectance curve from unit to unit that might be used in band ratioing techniques. It is particularly useful in this analysis, because the dry and moist non-saline soils show quite a range of absolute reflectances, but a relatively uniform normalized reflectance curve (Fig. 16).

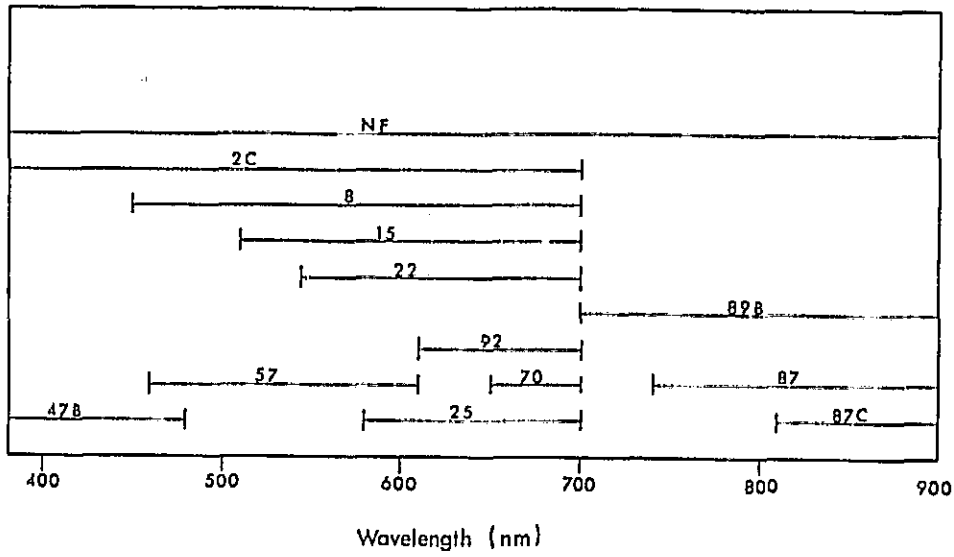


Figure 15. Bandpass filters used in spectral reflectance measurements.

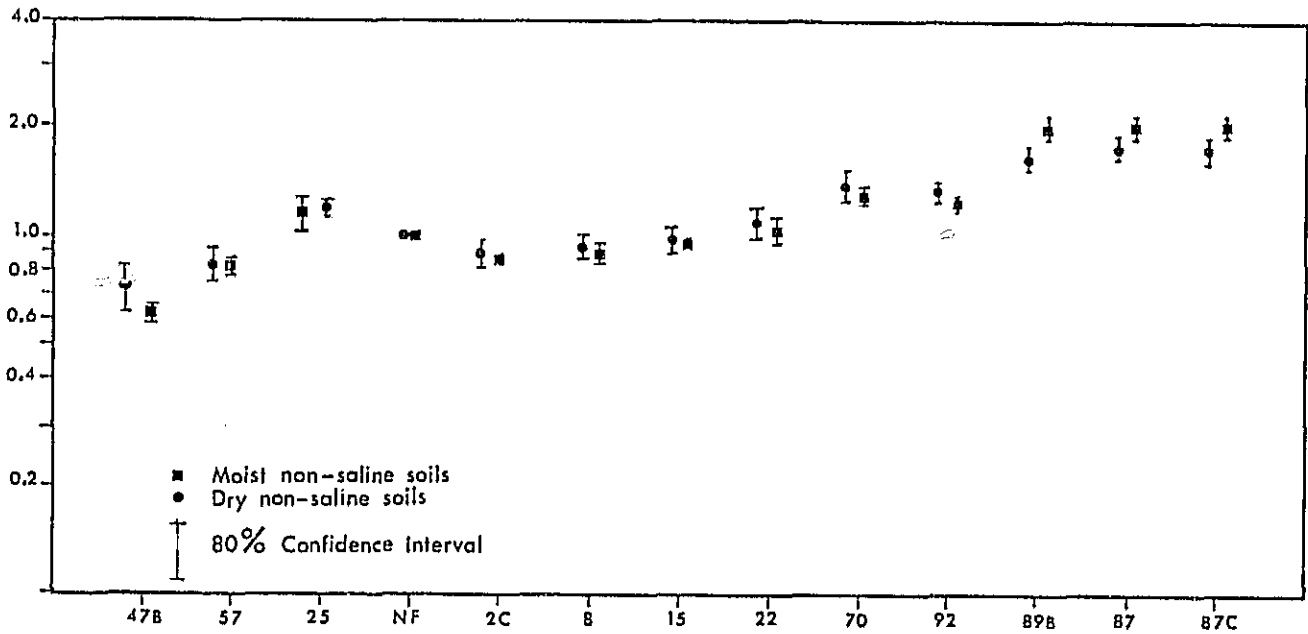


Figure 16. Normalized band reflectance of dry and moist non-saline soils.

REPRODUCTION OF THIS REPORT
 ORIGINAL PAGE IS UNCLASSIFIED

Figure 17 shows the normalized band reflectance plots for saline soils compared with moist and dry non-saline soils separately. Only the 47B (blue) band, the 2C (minus UV) band, and the 89B, 87B, 87C (photo-infrared) band show significant separations at the 80% confidence interval. The same effect in the infrared bands is observed in the plot of dry versus moist non-saline soils (Fig. 16), and it is suggested that saline soils having a high average reflectance show a reduced slope of increased reflectance towards the infrared region. These observations indicate that ratioing may help increase the contrast between high reflectance units, such as saline soils, from soils having the usual range of intermediate reflectances. This has not been tested in application.

A plot of absolute band reflectances for dry non-saline and saline soils is shown in Figure 18. There is separation of the ranges in the photo-infrared bands, the deep red bands, the minus-blue band, and the no-filter band. These observations contradict the subjective evaluation of S190A photography, where the infrared bands show the least contrast. One possible explanation for this, aside from the generally poor quality of the infrared bands, is that the photography is not contrasting non-saline with saline soils, but is contrasting vegetation with saline soils. Vegetation typically exhibits a high photo-infrared reflectance, which would show a low contrast with saline soils, and exhibits a much lower green-band reflectance than that measured for the saline soils. This may well affect the conclusions reached above concerning band ratioing.

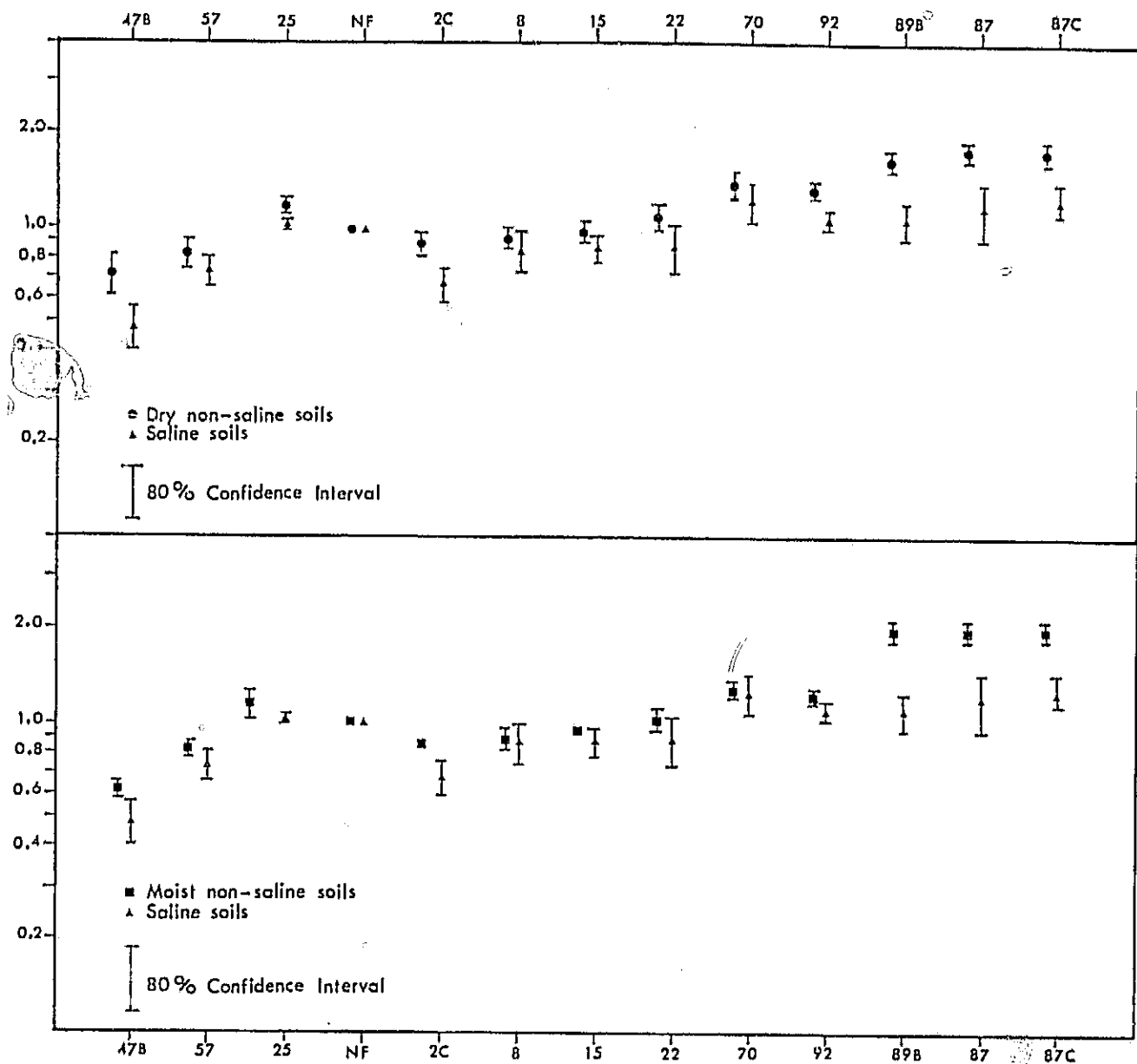


Figure 17. Normalized band reflectance of saline soils, and moist and dry non-saline soils.

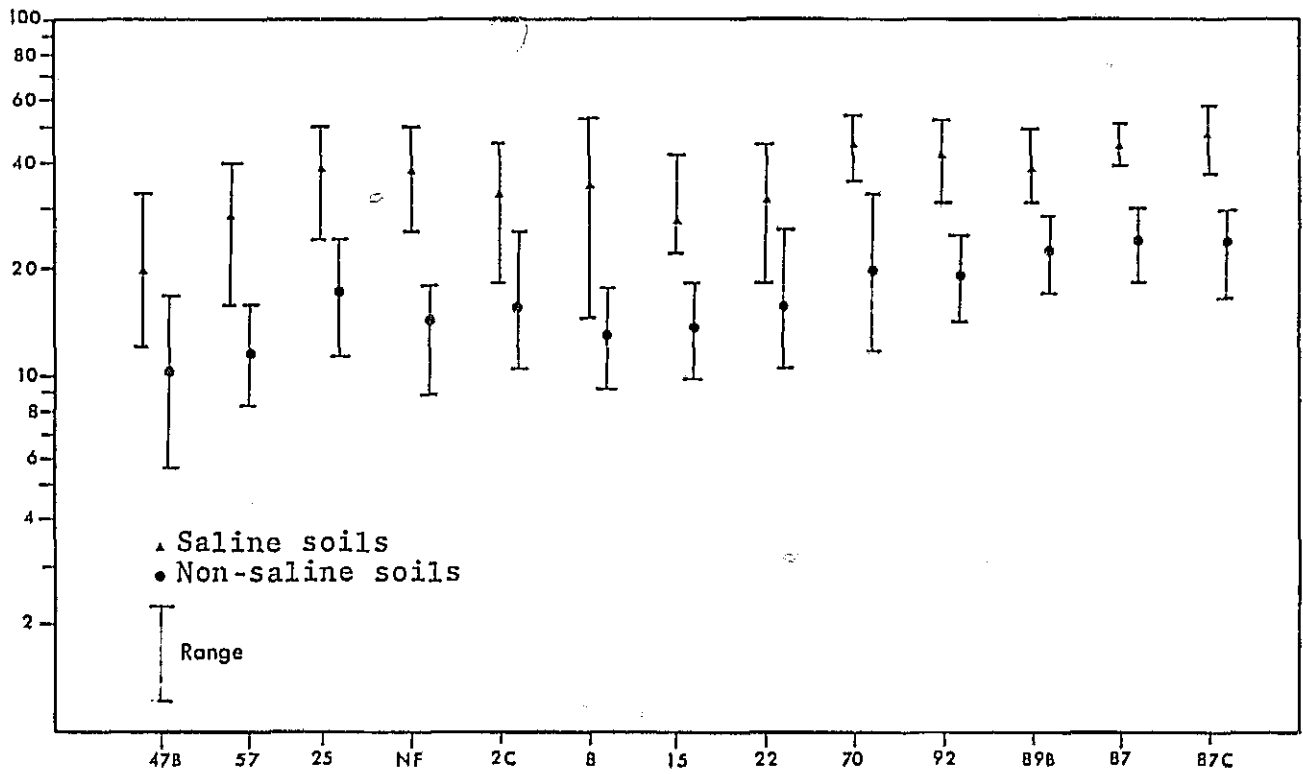


Figure 18. Absolute band reflectance (in percent) of saline and non-saline soils.

Summary and General Remarks

Narrowleaf cottonwood trees and willows are present only where water saturated material is present within 4m of the surface. This condition is met both where the water table is shallow and where streams have sufficient flow to maintain saturated bank sediments throughout the year, with either a shallow or deep water-table. Where the vegetation extends away from streams a good distance, the ground water table is likely shallow.

The presence of saline soil more reliably indicates shallow ground water, but it also is dependent upon the position within the regional flow system and the ground water quality. If non-saline and saline soils are being mapped, band ratioing may increase contrast. If vegetation and saline soils are being compared, as appears likely at satellite resolution, the green band shows better contrast than the other available bands.

EVAPOTRANSPIRATIVE DISCHARGE

Rates of evapotranspirative discharge from the water table depend upon vegetation density and type, ground water depth, and climate. The vegetation/land use map (Fig. 7) contains the essential vegetation information. This information, combined with ground water depth information (as discussed in the previous section) and climatic information,

allows a computation of evapotranspiration rates of an accuracy sufficient for most regional ground water studies. For this computation, both vegetation and soil salinity should be used as indicators of depth to a saturated zone, because evapotranspirative rates are equal for a shallow water table, a perched water table, and saturated stream bank sediments well above the water table.

CONCLUSIONS

1) Resolution is the single most important factor in determining the potential application of Skylab photography to hydrogeologic investigations.

2) Skylab S190A photography used in a stereo mode is sufficient for defining the drainage divides and drainage patterns at the regional level. This information, combined with geologic information, defines the boundaries and distribution of ground water recharge and discharge areas within the basin.

3) Only Skylab S190B photography has sufficient resolution to adequately map more than the most obvious hydrogeologic units and structures, and in some cases may be sufficient for regional studies. In most regions, however, aircraft photography is still a necessity to produce an accurate and useful hydrogeologic map. Field work is a necessity for all studies.

4) Both vegetation and soil salinity are useful indicators of shallow ground water, but both must be interpreted carefully.

5) Evapotranspirative rates can be interpreted through knowledge of the climate and use of vegetation and ground water depth information interpreted from Skylab photography.

REFERENCES

- Emery, P.A., Snipes, R.J., Dumeyer, J.M., and Klein, J.M., 1973, Water in the San Luis Valley, south-central Colorado: Colorado Water Conserv. Board Water Resources Circ. 18, 26 p.
- Freeze, R.A., 1969, Theoretical analysis of regional groundwater flow: Inland Waters Branch Scientific Series No. 3, Canadian Dept. of Energy, Mines, and Resources. 147 p.
- Huntley, David, 1973, Hydrogeology of the Crestone quadrangle area, Colorado: unpublished summary of research, Colorado School of Mines. 29 p.
- Mifflin, M.D., 1968, Delineation of groundwater flow systems in Nevada: Desert Research Institute, Univ. of Nevada, Tech. Rept. #4., 110 p.
- Raines, G.L., and Lee, Keenan, 1974, Spectral reflectance measurements: Photogrammetric Eng., v. 40, no. 5, p. 547-550.
- _____, 1975, In situ rock reflectance: Photogrammetric Eng., v. 41, no. 2, p. 189-198.
- Toth, J., 1963, A theoretical analysis of groundwater flow in small drainage basins: Jour. of Geophysical Research, v. 68, no. 16, p. 4795-4813.